Astron. Astrophys. 335, 959–968 (1998)

ASTRONOMY AND ASTROPHYSICS

The Li dip: a probe of angular momentum transport in low mass stars

Suzanne Talon[1] **and Corinne Charbonnel**[2]

[1] Département d'Astrophysique Stellaire et Galactique, Observatoire de Paris, Section de Meudon, F-92195 Meudon, France
[2] Laboratoire d'Astrophysique de Toulouse, CNRS UMR5572, OMP, 14, Av. E.Belin, F-31400 Toulouse, France
(Suzanne.Talon@obspm.fr, Corinne.Charbonnel@obs-mip.fr)

Received 9 September 1997 / Accepted 20 April 1998

Abstract. We use the measures of Li and rotational velocities in F Hyades stars to assess the role of the wind-driven meridian circulation and of shear turbulence in the transport of angular momentum in stars of different masses. Our models include both element segregation and rotation-induced mixing, and we treat simultaneously the transport of matter and angular momentum as described by Zahn (1992) and Maeder (1995).

We show that the hot side of the Li dip in the Hyades is well explained within this framework, which was also successfully used to reproduce the C and N anomalies in B type stars (Talon et al. 1997). On the cool side of the dip, another mechanism must participate in the transport of angular momentum; its efficiency is linked to the depth of the surface convection zone. That mechanism should also be responsible for the Sun's flat rotation profile.

Key words: hydrodynamics – turbulence – stars: abundances – stars: interiors – stars: rotation

1. Towards a consistent description of rotation induced mixing

During the last decade, special efforts have been devoted to improve the description of the mixing processes related to stellar rotation. The most recent works (see for example Pinsonneault et al. 1989, Zahn 1992, Maeder 1995, Talon & Zahn 1997) describe the evolution of the internal distribution of angular momentum in a self-consistent manner under the action of meridional circulation and of shear turbulence. The mixing of chemicals is then linked directly to the rotation profile, whereas previous studies made use merely of a parametric relation between the turbulent diffusivity and the rotational velocity (cf. e.g. Schatzman et al. 1981, Zahn 1983).

Such a self-consistent treatment was applied successfully by Talon et al. (1997) in the study of a 9 $M_\odot$ star, modeling the transport of angular momentum by the meridional circulation as a truly advective process. The only assumption in this theory is that the turbulence sustained by the shear is highly anisotropic and relies on two free parameters; the first one describes the magnitude of the horizontal shears (cf. Zahn 1992) and the second one, the erosion of the restoring force due to both the thermal and the mean molecular weight stratifications (cf. Maeder 1995, Talon & Zahn 1997). These authors reproduce the slight abundance anomalies measured in B stars by Gies & Lambert (1992). They also show that the widening of the main sequence, which is generally attributed to convective overshooting in massive stars, may be due to the rotational mixing present in stars having a "typical" velocity for the spectral type considered.

Concerning low-mass stars, it has been shown that the hydrodynamical models relying on meridional circulation and shear fail to reproduce the solar rotation profile given by the helioseismic observations (Brown et al. 1989, Kosovichev et al. 1997): at the solar age, those models still have large Ω gradients which are not present in the Sun (see Chaboyer et al. 1995 and Matias & Zahn 1997). That conclusion has been reached independently by two different groups, using different descriptions for the transport processes. On one hand, the Yale group computed the evolution of angular momentum in low mass stars with a simplified description of the action of the meridional circulation which was considered as a diffusive process rather than as an advective process. The whole evolution of momemtum and chemicals was then due to diffusion only, with a free parameter that had to be calibrated to differentiate the transport of the passive quantities with respect to that of vectorial ones. Pinsonneault et al. (1990) were then able to reproduce the surface Li abundances for low-mass cluster stars (with effective temperature lower than 6500K). However, they obtained large rotation gradients within these stars which are excluded by helioseismology (Chaboyer et al. 1995). On the other hand, Matias & Zahn (1997) performed a complete study for the evolution of the Sun's angular momentum, where they took into account the advective nature of the meridional circulation. They also concluded that meridional circulation and shear turbulence are not efficient enough to enforce the flat rotation profile measured by helioseismology.

These results indicate that another process participates in the transport of angular momentum in solar-type stars, while the so-called wind-driven meridional circulation (Zahn 1992) is successful in more massive stars. In order to study the transition

Send offprint requests to: Suzanne Talon, Present address: CERCA, 5160, boul. Décarie, bureau 400, Montréal (Québec) Canada H3X 2H9

between solar-type and more massive stars and to identify the mass range for which the present description for the transport of angular momentum and chemicals relying only on rotation fails, we propose to use the measures of lithium and rotational velocities in galactic cluster stars.

We first review the observations of lithium abundances and rotation in the Hyades main-sequence stars, and summarize the difficulties of the various models proposed so far to explain the Li dip in F stars (Sect. 2). We recall the equations that describe the evolution of angular momentum due to meridian circulation and shear turbulence as well as the associated transport of chemicals (Sect. 3). We study the impact of rotational mixing on the lithium abundance in galactic cluster F stars, and compare this to the observations. Our models include both element segregation and rotation-induced mixing, and we treat simultaneously the transport of matter and angular momentum. The internal rotation profile thus evolves completely self-consistently under the action of meridional circulation as described by Zahn (1992) (see also Matias et al. 1997), and of shear stresses which take into account the weakening effect of the thermal diffusivity, as was first shown by Townsend (1958) (Sect. 4). We show that the blue side of the lithium dip is well reproduced within this framework, and that the process responsible for the shape of the solar rotation profile should become efficient only for stars on the cool side of the Li dip, where the external convection zone is thick enough. By achieving efficiently momentum transport, the global effect of this process would be to reduce the mixing due to the rotational instabilities in stars with effective temperature lower than $\sim$ 6500K. The most likely candidates for this transport process are the gravity waves generated by the external convection zone (Schatzman 1993; Zahn et al. 1997; Kumar & Quataert 1997) and the large-scale magnetic field which could be present in the radiative interior (Charbonneau & MacGregor 1993; Barnes et al. 1997).

2. Lithium and rotation in the Hyades F-stars

Lithium (a fragile element which burns at relatively low temperature in stellar interiors) has traditionally been used as a very powerful tracer of particle transport processes. Many Li abundance determinations are available for stars of different spectral types in galactic clusters of various ages, together with observed rotational velocities in some cases (see for ex. Soderblom 1993, Balachandran 1995 and references therein).

Relying on [Li/Ca] observations in Hyades stars, Wallerstein et al. (1965) detected a drop-off in the lithium content of main sequence stars with a spectral index around (B-V)=0.4. It was clearly confirmed much later by Boesgaard & Tripicco (1986) that Li is indeed depleted in Hyades F-stars in a range of 300 K in effective temperature centered around 6600 K (cf. Fig. 1 top). On the blue side of the so-called "Boesgaard-dip", Li abundances drop sharply, while the rise on the red side is more gradual. Evidence of the same feature has been seen in all galactic clusters older than 10^8yr as well as in field stars (see Michaud & Charbonneau 1991 and Balachandran 1995 for a complete list of references).

The simplest explanation for this characteristic feature was proposed by Michaud (1986) who showed how chemical separation could shape the gap in the Hyades F stars. This model relied on well-known physics with two adjusted parameters: the mass loss rate needed to reduce the predicted over-abundances due to radiative acceleration on the hot side of the plateau and the ratio of the mixing length to the pressure scale height. Three observational facts however contradict the pure microscopic diffusion hypothesis. Firstly, the predicted width of the Li dip at the age of the Hyades is narrower than observed (Richer & Michaud 1993). Secondly, the carbon, oxygen and boron under-abundances expected in the case of pure diffusion (Michaud 1986, Turcotte et al. 1997) failed to be found in the Hyades F stars (Boesgaard 1989, Friel & Boesgaard 1990, García López et al. 1993) and in Li and Be deficient F field stars (Boesgaard et al. 1997). This indicates that a macroscopic process counteracts the effects of element segregation in these stars. Finally, in the pure diffusion model, Li settles and remains in a buffer zone below the convective envelope; it should then been dredged to the surface as soon as those stars leave the main sequence. Observations of lithium in M67's slightly evolved stars (Pilachowski et al. 1988; Balachandran 1995; Deliyannis et al. 1997) show however that the lithium depletion in stars formerly from the dip persists on the sub-giant branch. This strongly favors explanations relying on nuclear destruction of lithium.

Schramm et al. (1990) proposed an explanation relying on mass loss. The peeling of the outer layers of the stars could bring to the surface the regions where lithium has been depleted by pure nuclear destruction. However, the existence of Hyades and field F stars which still have some lithium but where some beryllium has been also depleted argues against that mechanism (Stephens et al. 1997).

Following Press' suggestion (1981) that gravity waves may induce shear mixing, García López & Spruit (1991) studied the transport of lithium as a function of spectral type. They found that low degree waves may become efficient sources of shear mixing for stars of the Li dip, as their production model is mainly dependent on the convective flux. A suitable choice of the mixing length then permits one to place the dip at the correct effective temperature (since it influences the disappearance of the convective zone). However, they needed to increase the efficiency of the wave generation by a factor of 15 over their estimation to correctly reproduce the dip. Furthermore, that model fails to reproduce the large abundance dispersion observed on the red side.

Boesgaard (1987) noticed that the Li dip in the Hyades coincides (in terms of effective temperature) with both a sharp drop in rotational velocities (see Fig. 1 bottom) and with the transition from high stellar activity to activity controlled by the stellar dynamo (Wolff et al. 1986). Rotation was then suggested to play a dominant role in the build up of the Li dip. Up to now, the different investigations of the possible connection between rotation and Li deficiencies in F stars have relied on highly simplified descriptions of the rotation-induced mixing processes. In the meridional circulation model of Tassoul & Tassoul (1982) used by Charbonneau & Michaud (1988), the feed-back effect

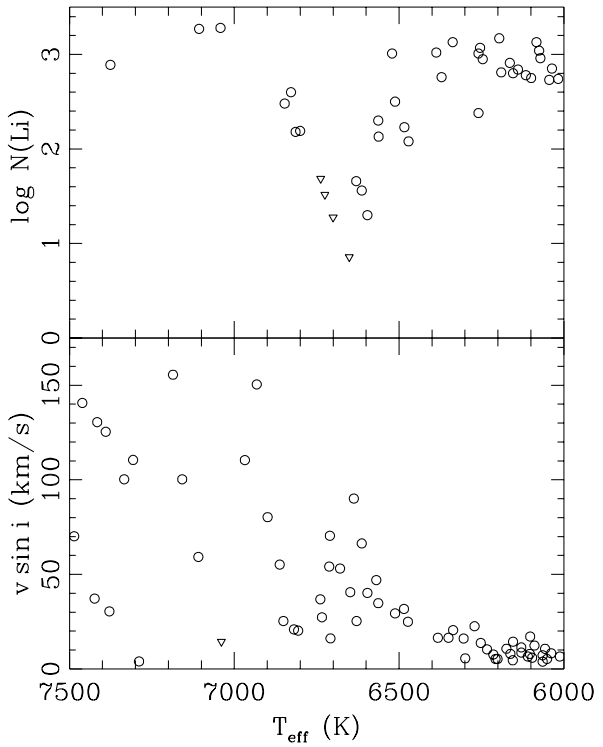

Fig. 1. (*top*) Lithium versus effective temperature in F Hyades stars (Boesgaard & Tripicco 1986, Thorburn et al. 1993). Triangles denote upper limits. (*bottom*) Projected rotational velocity versus effective temperature in F Hyades stars. Observational data are from Kraft (1965), Stauffer et al. (1987), and Mermilliod (1992).

due to angular momentum transport as well as the induced turbulence were ignored. Following Zahn (1992), Charbonnel et al. (1992, 1994) considered the interaction between meridional circulation and turbulence induced by rotation, but the transport of angular momentum was not treated self-consistently.

Here we go one step further by including in our models the most complete description currently available for rotation-induced mixing, and we compute simultaneously the transport of chemicals and the transport of angular momentum due to wind-driven meridional circulation. Let us stress again that this description has been used to successfully reproduce the slight over (under) abundances of C (N) observed in B type stars (cf. Talon et al. 1997) but failed to explain the flat rotation profile observed in the Sun (cf. Matias & Zahn 1997). Another process which efficiently transports angular momentum must be invoked in order to explain the helioseismic data. Here, we use the observations of lithium and rotation in the Hyades in order to get constraints on the onset of that process.

3. The transport processes: rotational mixing and microscopic diffusion

We calculate the destruction of lithium in F-type stars, assuming that rotational mixing is the only source of transport for angular momentum. The evolution of the interior radial differential rotation is calculated completely self-consistently, using the most complete description currently available for the following physical processes:

- the advection of angular momentum by the meridional flow driven by the thermal imbalance in a rotating star, assuming that the rotation velocity is homogenized on isobars by anisotropic shear turbulence, as described by Zahn (1992);
- the turbulent transport due to the vertical shear present in differentially rotating bodies, including the weakening effect of the thermal diffusivity on the density stratification (for details see e.g. Talon & Zahn 1997).

The complete equation for the transport of angular momentum is then

$$\rho \frac{\mathrm{d}}{\mathrm{d}t}\left[r^2\Omega\right] = \frac{1}{5r^2}\frac{\partial}{\partial r}\left[\rho r^4 \Omega U\right] + \frac{1}{r^2}\frac{\partial}{\partial r}\left[\rho \nu_v r^4 \frac{\partial \Omega}{\partial r}\right] \qquad (1)$$

where we use standard notations for the radius r and the density ρ and where ν_v is the vertical (turbulent) viscosity. $U(r)$ is the vertical component of the meridian velocity and is given by

$$U(r) = \frac{L}{Mg}\left(\frac{P}{C_P \rho T}\right)\frac{1}{\nabla_{\rm ad} - \nabla}\left[E_\Omega + E_\mu\right], \qquad (2)$$

where L is the luminosity, M the mass, g the gravity, P the pressure, C_P the specific heat at constant pressure and T the temperature. E_Ω and E_μ depend respectively on the rotation profile and on the mean molecular weight gradients (for the complete expression, see Zahn 1992). The expression of the turbulent viscosity is

$$\nu_v = \frac{2}{5} K \left(\frac{r}{N}\frac{\partial \Omega}{\partial r}\right)^2, \qquad (3)$$

where N is the Brunt-Väisälä frequency and K is the thermal diffusivity. The coefficient $\frac{2}{5}$ used here is the one that was found by Maeder (1995) when he rederived the criterion for shear instabilities assuming spherical geometry for the turbulent eddies. As was discussed by Talon & Zahn (1997), even though this is somewhat of an arbitrary choice, the exact value shouldn't differ much. In this study, we will use the value $\frac{2}{5}$ and not consider it as a free parameter.

Microscopic diffusion of lithium, helium and metals, including gravitational and thermal settling, is taken into account (see Appendix for a description of the corresponding input physics).

Modeling the combination of the advective transport by the circulation and the strong horizontal diffusion D_h present in stratified media by an effective diffusivity $D_{\rm eff}$ (cf. Chaboyer & Zahn 1992):

$$D_{\rm eff} = \frac{|rU(r)|^2}{30\, D_h}, \qquad (4)$$

the evolution of a chemical concentration c_i is given by:

$$\rho\frac{\partial c_i}{\partial t} = \dot{c}_i + \frac{1}{r^2}\frac{\partial}{\partial r}\left[r^2 \rho\, U_{\rm diff}\, c_i\right] + \frac{1}{r^2}\frac{\partial}{\partial r}\left[r^2 \rho \left(D_{\rm eff} + D_{\rm turb}\right)\frac{\partial c_i}{\partial r}\right], \qquad (5)$$

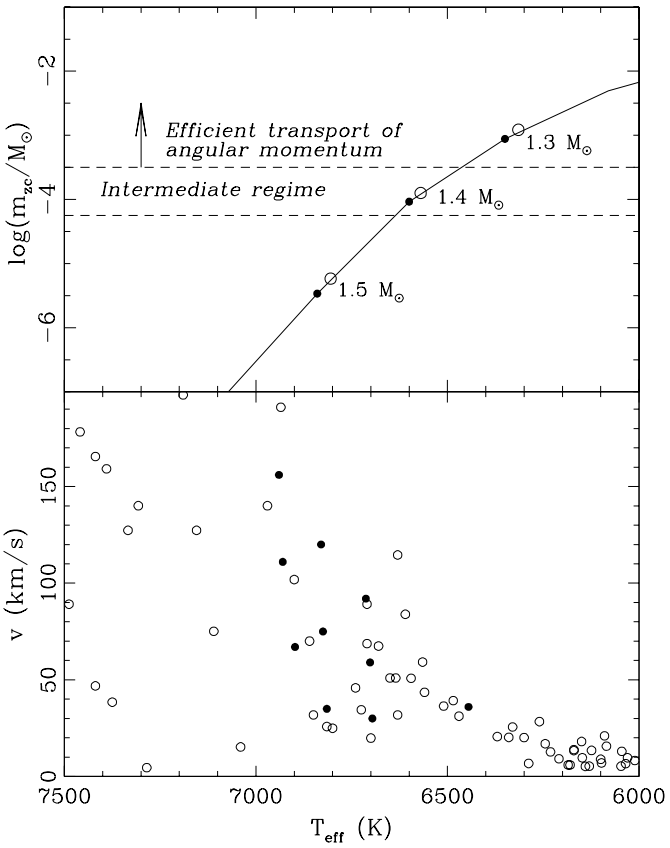

Fig. 2. (*top*) The size of the convective envelope (m_{zc}) at the age of the Hyades is plotted as a function of the stellar effective temperature. The filled dots represent standard models (i.e., non rotating); the open dots correspond to rapidly rotating models (150 km/s, not spun down at the age of the Hyades). Fast rotators have lower effective temperatures and deeper convective envelopes than the standard models. (*bottom*) Rotational velocities of our models at the age of the Hyades (filled dots; see Table 1). Also shown are the measured projected velocities times $4/\pi$ (open dots).

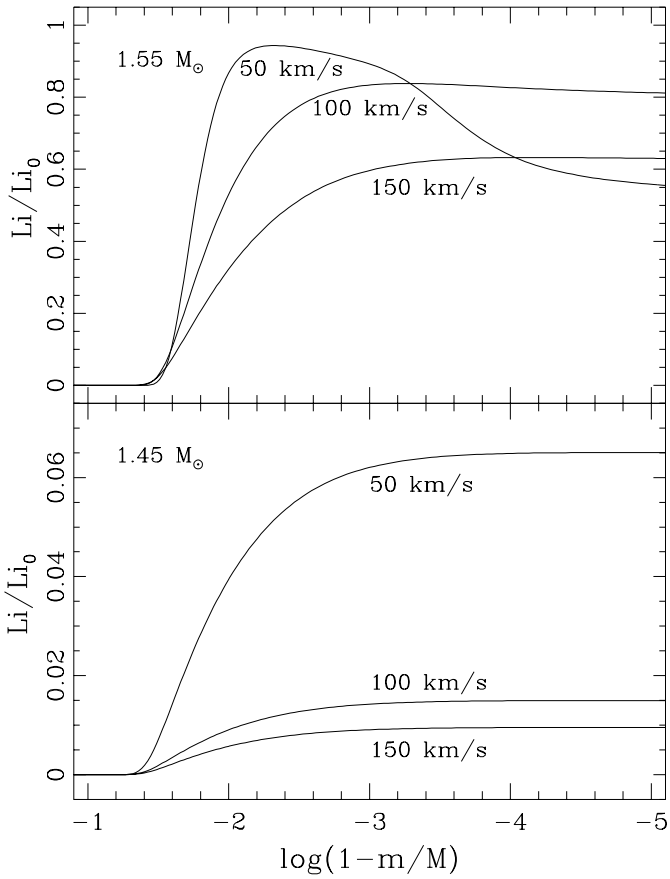

Fig. 3. Interior Li profile at the age of the Hyades for two different masses (1.55 and 1.45 $M_\odot$) and three different initial velocities (50, 100 and 150 km/s). The 1.55 $M_\odot$ model is not spun down and conserves its initial angular momentum; only the slower model feels the effect of microscopic diffusion, while rotation induced mixing dominates below the convection zone of the fastest models. The 1.45 $M_\odot$ model is strongly spun down and Li destruction is large for all values of the initial velocity.

where $\dot{c}_i$ is the nuclear production/destruction rate and $U_{\rm diff}$ is the microscopic diffusion; we assume $D_{\rm turb} = \nu_v$. The weakest point is this model is the magnitude of the horizontal diffusion coefficient. Here, we will use a parametric relation which links that coefficient to the advection of momentum:

$$D_h = \frac{rU}{C_h}\left[\frac{1}{3}\frac{{\rm d}\ln \rho r^2 U}{{\rm d}\ln r} - \frac{1}{2}\frac{{\rm d}\ln r^2\Omega}{{\rm d}\ln r}\right], \quad (6)$$

where C_h is an unknown parameter of order unity (see Zahn 1992 for more details).

4. The efficiency of rotational mixing in F-stars

4.1. Constraints from the observed surface rotation in galactic cluster F stars

As can be seen in Fig. 1, the stars of the Li dip are peculiar as far as their rotational history is concerned. From the observational data, one may conclude that the physical processes responsible for the surface velocity are different or operate with different time scales when one goes to lower effective temperature: stars hotter than $\sim$ 6900 K still have their initial velocities (when compared to the velocity distribution observed in younger clusters) while stars cooler than $\sim$ 6400 K have been very efficiently spun down at the age of the Hyades (700 Myr).

This behavior is linked to the variation of the thickness of the external convection zone (Fig. 2 top). Indeed, the hottest stars have only a very shallow surface convection zone which is not an efficient site for magnetic generation via a dynamo process. The coolest stars have a deeper surface convection zone, thus sustaining a strong magnetic field which spins down the outer layers efficiently. The rapid diminution with increasing effective temperature in the efficiency of magnetic braking observed for stars of the Li dip is a clear signature of the rapid decrease in mass of the envelope convection zone in stars of the corresponding effective temperature. Let us note that the diminution of the moment of inertia of the convective envelope as the effective temperature increases implies an even more drastic change in

Table 1. Characteristics of the stellar models, rotation velocities and lithium and beryllium depletion factors at the ages of the considered galactic open clusters. The models are computed with [Fe/H] of the Hyades (+0.12)

M_* ($M_\odot$)	t (Myr)	$T_{\rm eff}$ (K)	$\log(L_*/L_\odot)$	$\log(m_{zc}/M_*)$	T_{zc} (10^6 K)	v (km s^{-1})	Li/Li_0	Be/Be_0
1.55	50	7045	0.71	-7.5	0.084	70	0.57	0.62
	100	7040	0.71	-7.5	0.079	70	0.30	0.35
	300	6990	0.72	-7.5	0.081	70	0.31	0.36
	450	6950	0.73	-7.3	0.087	70	0.44	0.48
	700	6900	0.75	-6.8	0.12	65	0.54	0.58
	50	7045	0.71	-7.5	0.084	120	0.53	0.57
	100	7035	0.71	-7.5	0.082	120	0.45	0.49
	300	7020	0.73	-7.1	0.099	115	0.78	0.81
	450	6985	0.74	-7.0	0.11	110	0.82	0.85
	700	6925	0.75	-6.6	0.13	110	0.79	0.85
	50	7045	0.71	-7.5	0.083	165	0.54	0.57
	100	7050	0.71	-7.3	0.093	165	0.80	0.83
	300	7025	0.73	-7.1	0.11	160	0.89	0.90
	450	7000	0.74	-7.0	0.11	155	0.82	0.90
	700	6940	0.75	-6.7	0.12	155	0.60	0.83
1.5	50	6900	0.64	-5.8	0.23	45	0.96	0.99
	100	6900	0.65	-5.8	0.23	45	0.85	0.98
	300	6880	0.66	-5.8	0.22	40	0.43	0.82
	450	6860	0.67	-5.7	0.23	40	0.26	0.66
	700	6815	0.69	-5.6	0.24	35	0.12	0.46
	50	6900	0.64	-5.8	0.23	95	0.89	0.99
	100	6900	0.65	-5.8	0.23	90	0.74	0.96
	300	6880	0.66	-5.8	0.22	85	0.35	0.74
	450	6865	0.67	-5.8	0.22	80	0.19	0.56
	700	6825	0.69	-5.6	0.23	75	0.076	0.35
	50	6900	0.64	-5.8	0.23	145	0.85	0.98
	100	6900	0.65	-5.8	0.23	140	0.69	0.95
	300	6885	0.66	-5.8	0.22	130	0.30	0.69
	450	6865	0.67	-5.8	0.22	125	0.16	0.50
	700	6830	0.69	-5.7	0.23	120	0.060	0.30
1.45	50	6745	0.58	-4.9	0.36	45	0.96	0.99
	100	6745	0.58	-4.9	0.36	45	0.83	0.98
	300	6735	0.59	-4.9	0.36	35	0.35	0.76
	450	6725	0.60	-4.9	0.36	35	0.17	0.55
	700	6695	0.62	-4.8	0.36	30	0.058	0.32
	50	6745	0.58	-4.9	0.36	90	0.89	0.99
	100	6745	0.58	-4.8	0.36	85	0.68	0.95
	300	6740	0.59	-4.8	0.36	70	0.18	0.55
	450	6725	0.60	-4.8	0.35	65	0.063	0.32
	700	6700	0.62	-4.8	0.36	60	0.012	0.14
	50	6745	0.58	-4.9	0.36	140	0.84	0.98
	100	6745	0.58	-4.9	0.36	130	0.60	0.91
	300	6740	0.59	-4.9	0.35	110	0.12	0.48
	450	6730	0.60	-4.9	0.35	105	0.040	0.25
	700	6715	0.62	-4.9	0.34	90	0.008	0.10
1.35	50	6470	0.43	-3.5	0.74	80	0.98	0.99
	100	6470	0.44	-3.6	0.72	70	0.96	0.97
	300	6465	0.45	-3.6	0.70	50	0.89	0.91
	450	6460	0.46	-3.6	0.68	40	0.83	0.86
	700	6445	0.47	-3.6	0.67	35	0.74	0.77

the magnitude of the magnetic torque than the variation of the surface velocities indicate.

We calculate Li destruction in models of different stellar masses within the theoretical framework described in Sect. 3.

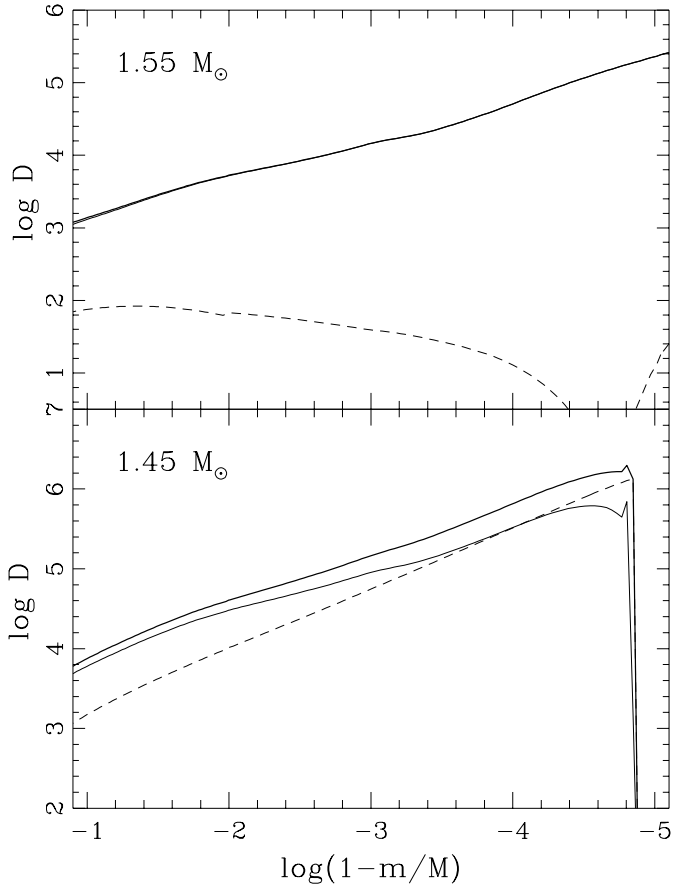

Fig. 4. Interior profile of the diffusion coefficient at the age of the Hyades and for an initial velocity of 100 km/s. The wide full line represents the total diffusion coefficient, the thin full line, the turbulent diffusion coefficient (cf. Eq. 3) and the dashed line, the effective diffusion coefficient (cf. Eq. 4). The 1.55 $M_\odot$ model is in the asymptotic regime, and it is turbulence which dominates the transport of chemicals whereas the transport of angular momentum by turbulence and meridional circulation is of equal magnitude and opposite signs. For the 1.45 $M_\odot$ model, while the transport of angular momentum is done mainly by the circulation, the transport of chemical is dominated by the former only close to the surface.

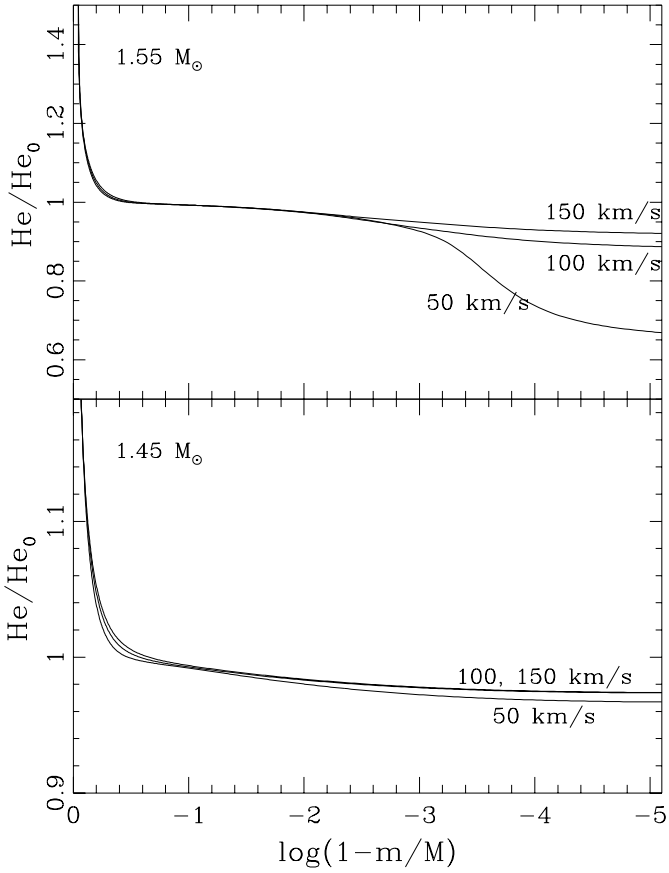

Fig. 5. Interior He profiles at the age of the Hyades, for the same models and rotation velocities as in Fig. 3.

We use the statistical study of rotation velocities in the Hyades performed by Gaigé (1993) in order to estimate the spin down associated to stars of different masses: we take an initial velocity of 100 km/s that corresponds to the mean velocity of hot stars ($T_{\rm eff} > 7000$ K) and that is consistent with velocities of cooler stars measured in younger clusters. The resulting velocity at the age of the Hyades (Fig. 2 bottom) corresponds to the average value for stars of a given effective temperature. We also calculate the dispersion expected in the Li abundances from different rotational histories using the $\pm 1\sigma$ values from Gaigé's study. The corresponding initial velocities are 50 and 150 km/s. The main characteristics of the stellar models, together with the rotation velocities and the lithium and beryllium depletion factors at different ages (corresponding to the ages of the clusters shown in Figs. 6 and 7) are given in Table 1.

4.2. The depletion on the blue side of the Li dip

Stars hotter than ∼6900 K

According to the observations, stars hotter than ∼6900 K are not slowed down by a magnetic torque. Since Eq. (1) admits a stationary solution, those stars soon reach a regime with no net angular momentum flux, in which meridional circulation and shear turbulence counterbalance each other. The weak mixing resulting from these processes is just sufficient to counteract the effect of microscopic diffusion, except in the slowest rotators in which its signature is visible (cf. Fig. 3 top and Fig. 4 top for the shape of the diffusion coefficients in the 1.55$M_\odot$ model). In our calculations of microscopic diffusion, only gravitational settling was included whereas in these stars, lithium may be supported by radiative acceleration (Michaud 1986). In improved radiative force calculations, Richer et al. (1997) showed however that the actual force on Li critically depends on the helium and metals abundance; in the dip region, gravitational settling of helium is needed for lithium to be supported against gravity. As can be seen in Fig. 5, the mixing strongly slows down the diffusion of helium in the external layers of the star. This may lead to a significantly reduction of the radiative acceleration on Li on the hot side compared to previous estimations. In any case, the main effect is that turbulence considerably reduces

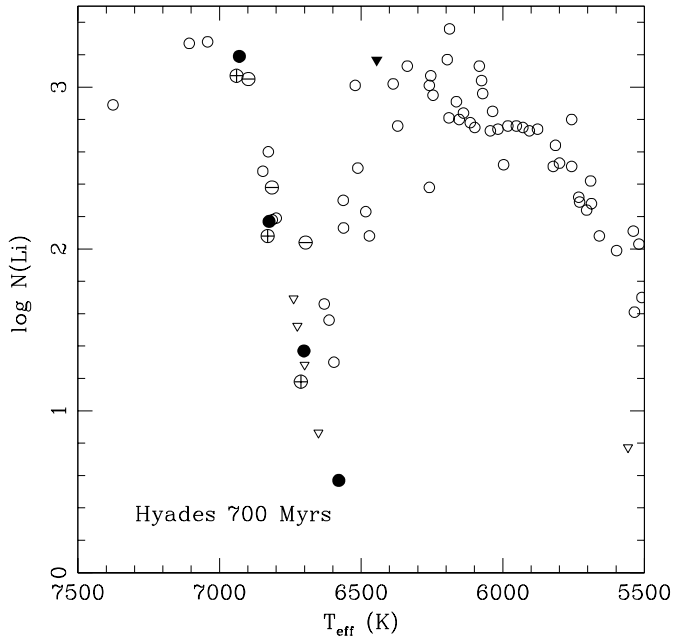

Fig. 6. Comparison of the models (filled dots and triangle, pluses and minuses) with the observations in the Hyades (open dots and triangles). The model with $T_{\rm eff} \simeq 6900$ K conserves its global angular momentum during its main sequence life while for models with $6500 < T_{\rm eff}({\rm K}) < 6900$, angular momentum is lost at the surface. Interior redistribution of momentum takes place only through rotational mixing; the coolest model ($T_{\rm eff} \simeq 6450$ K) is computed assuming solid body rotation. The filled dots correspond to numerical calculations performed with an initial velocity of 100 km/s, the pluses to an initial velocity of 150 km/s, and the minuses to initial velocity of 50 km/s. The corresponding rotational velocities at the age of the Hyades are shown in Fig. 2 (see also Table 1). Numerical calculations are performed using a value of [Fe/H]=+0.12, i.e., that of the Hyades.

microscopic diffusion, and leads only to small variations in the surface abundances.

Stars with 6600$< T_{\rm eff}({\rm K}) <$6900

In this effective temperature range, a weak magnetic torque slows down the outer layers of the stars. As the magnetic torque increases with diminishing temperatures, meridional circulation has much more angular momentum to transport to the surface, leading to a larger destruction of Li (cf. Fig. 3 bottom and Fig. 4 bottom for the shape of the diffusion coefficients in the $1.45 M_\odot$ model). Again, Li is transported by meridional circulation, shear turbulence and microscopic diffusion. Let us note however that here, the gap is not shaped by element segregation, as in Michaud (1986) but by the properties of braking and angular momentum transport. Furthermore, since here Li is destroyed and not barely hidden below the convection zone, no dredge-up of this element is expected due to the deepening of the external convection zone when the stars will leave the main sequence. This is in agreement with the absence of Li detection in Balachandran's (1995) sub-giants.

The predictions for the lithium abundance at different ages are given in Figs. 6 and 7, and compared to observations in galactic clusters. We also show predictions for models with [Fe/H]=-0.15 in Fig. 7, in order to take into account the metallicity differences between the various clusters. At the age of the Hyades, rotational mixing described in Sect. 3 perfectly explains the shape of the blue side of the Li dip, as well as the observed dispersion. This clearly indicates that, in this effective temperature range, the process which participates to the transport of angular momentum in the Sun is not yet efficient.

We computed the effect of rotational mixing on beryllium, which burns at a slightly higher temperature than lithium ($\sim 3.5 \cdot 10^6$K instead of $\sim 2.5 \cdot 10^6$K). At the age of the Hyades, the surface beryllium abundance has diminished by as much as a factor 5 in the center of the dip. This is in agreement with the observations by Boesgaard & Budge (1989) in the Hyades and by Stephens et al.(1997) in field stars, as can be seen in Fig. 8. However, the comparison with Stephens' data is marginal because of the inhomogeneity in metallicity and evolutionary status of their sample. New observational data, with modern detectors, would be necessary for beryllium in more stars of the Li dip.

4.3. The red side of the Li dip

Stars with 6400$< T_{\rm eff}({\rm K}) <$6600

On the red side of the dip, the magnetic torque strengthens as the convective zone grows (Fig. 2). If we assume there that all the momentum transport is assured by the wind-driven meridional circulation, and if we keep the same parameters that explain the Li abundances on the blue side of the dip as well as the chemical anomalies in more massive stars, we obtain too much lithium burning compared to the observations in this cool effective temperature domain (cf. Fig. 6, model with $T_{\rm eff} \simeq 6550$ K). Even though a different calibration of the free parameters may lead to the observed lithium abundances, it would not change the internal rotation profile which is known to be inconsistent in the solar case.

We rather propose that the red side of the dip corresponds to a transition region where some other physics for angular momentum transport, which is known to be present in the Sun, starts to become efficient. In that case, the magnitude of both the meridional circulation and shear turbulence is reduced, as well as the Li depletion by rotation-induced mixing. We suggest that this increase of efficiency is linked to the growth of the surface convection zone (see Fig. 2 top). This efficient transport mechanism for angular momentum could be due to gravity waves or to a magnetic field in the radiative interior (see references given in the first part).

A complete description of the efficient mechanism for the transport of angular momentum is required in order to calculate self-consistently the Li destruction in this region, and has not been attempted here.

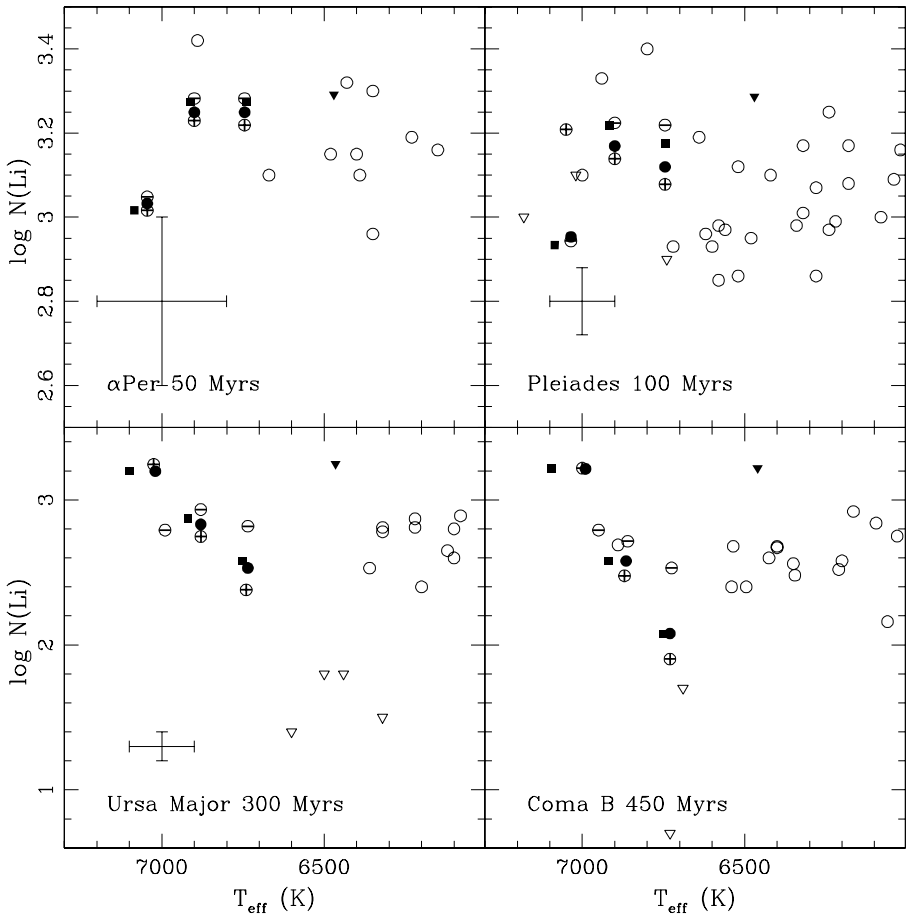

Fig. 7. Shape of the Li dip at the age of different galactic clusters. Symbols are as in Fig. 6. Filled squares denote calculations made for a metallicity of [Fe/H]=−0.15 and an initial velocity of 100 km/s. Typical observational error bars are shown when available.

Stars cooler than $\sim$ 6400 K

The maximum of the Li abundance at $\sim$ 6400 K indicates that the "extra" process reaches there its full efficiency, which must be sufficient to lead to solid body rotation in the Sun (at the solar age). We stress once more that a self-consistent calculation of Li destruction requires a description of that mechanism. It is however possible to estimate the lower limit of Li destruction by calculating the meridional circulation present in solid body rotators (filled triangles in Figs. 6, 7 and 8); this must be viewed only as an upper limit on the Li abundance for stars of this domain.

Two important remarks have to be done on the transition region.

Firstly, it was shown by Balachandran (1995) that the location of the Li dip in different clusters depends on the effective temperature *on the ZAMS* and is thus independent of metallicity. Our explanation is entirely consistent with this observation[1] since for low mass stars, the size of the external convection zone is directly related to the effective temperature. It is then the former which controls magnetic activity (and thus, the spin-down) as well as the onset of the "efficient" mechanism for angular momentum transport.

Secondly, the measures of Li abundances in the Hyades stars of $6600 \gtrsim T_{\rm eff}({\rm K}) \gtrsim 6200$ exhibit a large dispersion while it is much smaller in cooler stars. This can be again linked to different rotational histories of stars of the same mass. Indeed, when these are young, the fast rotators have a larger convective zone than their slower counterparts (see Table 1 and Fig. 2 top). Therefore, in the early stages meridional circulation could be lower than expected, leading to a smaller Li destruction. Even though the magnitude of this change of m_{zc} may seem small, it is not negligible compared to the size of the transition region. A detailed description of angular momentum transport by the "efficient" process is however required in order to quantify the magnitude of this effect.

5. Conclusions

Assuming rapid rotation and using a self-consistent description for the transport of angular momentum and of chemicals by meridional circulation and shear instabilities (cf. Zahn 1992, Talon & Zahn 1997), Talon et al. (1997) successfully explained the C and N anomalies observed in some B stars.

At the same time, it was shown (Matias & Zahn 1997) that this description applied to the transport of angular momentum in the Sun is incomplete, leading to large Ω gradients which are not observed. Another transport mechanism must thus be invoked in low mass stars.

[1] Let us note that this is also the case for several of the mechanisms which have been suggested so far, for the reason mentioned here.

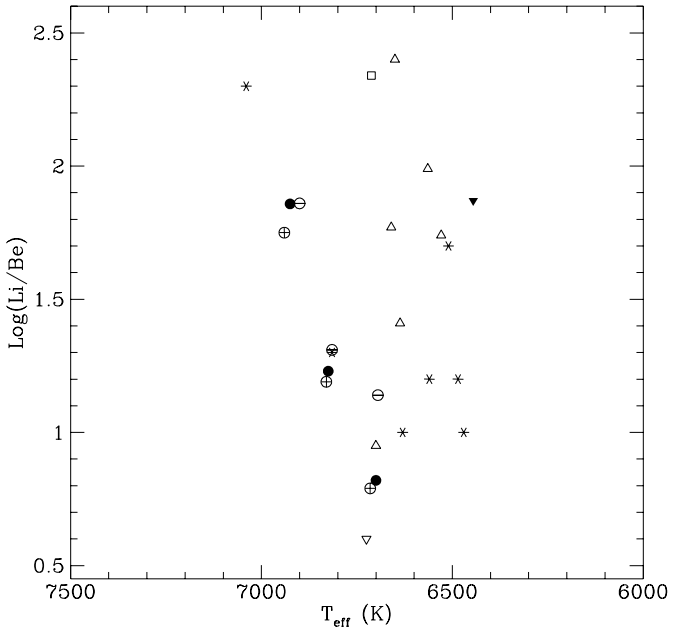

Fig. 8. Logarithm of the lithium to beryllium ratio as a function of the effective temperature. The predictions are given with the same symbols as in Fig. 6. The asterisks and inverted triangles correspond to the observations and upper limits in the Hyades (Boesgaard & Budge 1989), and the square and triangles to observations and upper limits in field stars with [Fe/H] between +0.09 and -0.39 (Stephens et al. 1997)

At this point, 2 questions remain: firstly, the nature of that transport mechanism has to be determined unambiguously and secondly, the location of the transition between the regime which is relevant for massive stars and the one which is relevant for low mass stars has to be identified.

In this paper, we addressed that second question. We presented numerical calculations of Li destruction due to rotational mixing using the *same* description as Talon et al. used for more massive stars and the same free parameters. We showed that this clearly reproduces the hot side of the Li dip. Let us recall that the destruction of lithium is then due solely to rotational mixing enhanced by the spin down of the outer layers. Stars hotter than 7000 K also undergo rotational mixing, but it is much milder due to the weak differential rotation.

The rise of Li abundances on the right side of the dip is not explained within this framework. We propose that it is linked to the appearance of another transport mechanism for angular momentum which reduces the magnitude of the meridional circulation and shears, leading to the observed diminution of Li destruction on the red side of the Li dip. This mechanism is known to occur in the Sun where it is responsible for the flat rotation profile.

Acknowledgements. We would like to thank Jean-Paul Zahn for his careful reading of this manuscript. This work was supported by grants from the GDR 131 "Structure Interne des Etoiles et Planètes Geantes" (CNRS). S.T. gratefully acknowledges support from NSERC of Canada and from the French Ministère des Affaires Étrangères.

Appendix A: input physics

The calculations are performed with the Toulouse-Geneva stellar evolution code, in which the equations described in Sect. 3.1 have been implemented. Transport processes are engaged on the arrival on the zero age main sequence. The stellar models were obtained with the following input micro-physics:

- Microscopic diffusion: The tables of collision integrals by Paquette et al. (1986) are used to calculate the diffusion coefficients.
- Opacities: The radiative opacities for the interior are taken from Iglesias & Rogers (1996). The low-temperature opacities are from Alexander & Ferguson (1994) which account for a wide variety of atomic and molecular species.
- Nuclear cross-sections: All the thermonuclear reaction rates are due to Caughlan & Fowler (1988), with the exception of the ^{17}O(p,γ)^{18}F and ^{17}O(p,α)^{14}N for which we adopt the values from Landré et al. (1990). Screening factors for the reaction rates are taken into account according to the analytical prescription by Graboske et al. (1973).
- Abundances: We use the proto-solar lithium abundance derived from carbonaceous chondrites by Anders & Grevesse (1989), log N(Li)=3.31$\pm$0.04, as cosmic value. This Li abundance is consistent with the photospheric Li abundances in F stars of young open clusters like αPer (Balachandran et al. 1996) and the Pleiades (Soderblom et al. 1993).

  We use [Fe/H]=+0.12 (Cayrel de Strobel et al. 1997) for the logarithm of the number abundances of iron to hydrogen relative to the solar values. The initial helium content is determined by $Y = 0.227 + (\Delta Y/\Delta Z)Z$, where the value for $\Delta Y/\Delta Z$ we use (2.524) was obtained by calibration of the solar models with the micro-physics described above and a solar metal abundance Z/X=0.0244 (Grevesse & Noels 1993). The relative ratios for the heavy elements correspond to the mixture by Grevesse & Noels (1993). We take the same isotopic ratios than Maeder (1983).
- Convection: Turbulent convection is described by the classical mixing-length theory of Böhm-Vitense (1958). Calibration of the solar model gave us a value of 1.6 for the free parameter α, ratio of the mixing-length to the pressure scale height. Neither overshooting, nor convective penetration have been considered in this work.

References

Alexander D.R., Fergusson J.W., 1994, ApJ 437, 879
Anders E., Grevesse N., 1989, in "Abundances of the elements - Meteoritic and solar", Ed., p.197
Balachandran S., 1995, ApJ 446, 203
Balachandran S., Lambert D.L., Stauffer J.R., 1996, ApJ 470, 1243
Barnes G., Charbonneau P., MacGregor K.B., 1997, ApJ (preprint)
Boesgaard A.M., 1987, PASP 99, 1067
Boesgaard A.M, 1989, ApJ 336, 798
Boesgaard A.M, Budge K.G., 1989, ApJ 338, 875
Boesgaard A.M., Deliyannis C.P., Stephens A., Lambert D.L., 1997, in "Cools stars, stellar system and the Sun", Eds. R.A. Donahue, J.A. Bookbinder

Boesgaard A.M., Tripicco M.J., 1986, ApJ 302, L49
Böhm-Vitense E., 1958, Zs.f.Ap. 46, 108
Brown T.M., Christensen-Dalsgaard J., Dziembowski W.A., Goode P., Gough D.O., 1989, ApJ 343, 526
Caughlan G.R., Fowler W.A., 1988, Atomic Data Nuc. Data Tables 40,283
Cayrel de Strobel G., Soubiran C., Friel E.D., Ralite N., Francois P., 1997, A&AS 124, 299
Chaboyer B., Zahn J.-P., 1992, A&A 253, 173
Chaboyer B., Demarque P., Pinsonneault M.H., 1995, ApJ 441, 865
Charbonneau P., Michaud G., 1988, ApJ 334, 746
Charbonneau P., MacGregor K.B., 1993, ApJ 417, 762
Charbonnel C., Vauclair S., Zahn J.P., 1992, A&A 255, 191
Charbonnel C., Vauclair S., Maeder A., Meynet G., Schaller G., 1994, A&A 283, 155
Deliyannis C.P., King J.R., Boesgaard A.M., 1997, in "Wide-Field Spectroscopy", Eds.E.Kontizas et al., p.201
Friel E.D., Boesgaard A.M., 1990 ApJ 351, 480
Gaigé Y., 1993, A&A 269, 267
García López R.J., Spruit H.C., 1991, ApJ 377, 268
García López R.J., Rebolo R., Herrero A., Beckman J.E., 1993, ApJ 412, 173
Kraft R.P., 1965, ApJ 142, 681
Gies D.R., Lambert D.L., 1992, ApJ 387, 673
Graboske H.C., de Witt H.E., Grossman A.S., Cooper M.S., 1973, ApJ 181, 457
Grevesse N., Noels A., 1993, in "Origin and Evolution of the Elements", Eds. Prantzos N., Vangioni-Flam E., Cassé M.
Iglesias C.A., Rogers F.J., 1996, ApJ 464, 943
Kosovichev A.G., et al., 1997, Solar Physics 170, 43
Kumar P., Quataert E.J., 1997, ApJ 475, L143
Landré V., Prantzos N., Aguer P., Bogaert G., Lefevre A., Thibaud J.P., 1990, A&A 240, 85
Maeder A., 1983, A&A 120, 113
Maeder A., 1995, A&A 299, 84
Matias J., Talon S., Zahn J.-P., 1997, A&A, preprint
Matias J., Zahn J.-P., 1997, in "Sounding solar and stellar interiors", IAU Symposium 181, Nice, in press
Mermillod J.C., 1992, private communication
Michaud G., 1986, ApJ 302, 650
Michaud G., Charbonneau P., 1991, Space Sci. Rev., 57, 1
Paquette C., Pelletier C., Fontaine G., Michaud G., 1986, ApJS 61, 177
Pilachowski C.A., Saha A., Hobbs L.M., 1988, PASP 100, 474
Pinsonneault M.H., Kawaler S.D., Sofia S., Demarque P., 1989, ApJ 338, 424
Press W.H., 1981, ApJ 245, 286
Richer J., Michaud G., 1993, ApJ 416, 312
Richer J., Michaud G., Massacrier G., 1997, A&A 317, 968
Schatzman E., Maeder A., Angrand F., Glowinski R., 1981, A&A 96, 1
Schatzman E., 1993, A&A 279, 431
Schramm D.N., Steigman G., Dearborn D.S.P., 1990, ApJ 359, L55
Soderblom D.R., 1993, Bull. of the AAS, 183, #17.14
Soderblom D.R., Jones B.F., Balachandran S. et al., 1993, AJ 106, 1059
Stauffer J.R., Hartmann L.W., Latham D.W., 1987, ApJ 320, L51
Stephens A., Boesgaard A.M., King J.R., Deliyannis C.P., 1997, ApJ 491, 339
Talon S., Zahn J.-P., 1997, A&A 317, 749
Talon S., Zahn J.-P., Maeder A., Meynet G., 1997, A&A 322, 209
Tassoul J.-L., Tassoul M., 1982, ApJS 49, 317
Thorburn J., Hobbs L.H., Deliyannis C.P., Pinsonneault M.H., 1993, ApJ 415, 150
Townsend A.A., 1958, J. Fluid Mech. 4, 361
Wallerstein G., Herbig G.H., Conti P.S., 1965, ApJ 141, 610
Wolff S.C., Boesgaard A.M., Simon T., 1986, ApJ 310, 360
Zahn J.-P., 1983, in "Astrophysical Processes in Upper Main Sequence Stars", 13^{th} Saas-Fee Course, Eds. B. Hauck, A. Maeder
Zahn J.-P., 1992, A&A 265, 115
Zahn J.-P., Talon S., Matias J., 1997, A&A 322, 320